Astigmatism on VLBA Antennas

VLBA Test Memo. No. 59

Bryan Butler

October 7, 1998

Introduction

For some time now, there have been various indications that the VLBA antennas are suffering from at least moderately serious astigmatism. Holography experiments gave a qualitative sense that this was the case. Beam cuts on LES-8 (Dhawan & Kestevan unpublished) definitely showed classic signs of astigmatism (filled in nulls, and which null was filled in [Az or El] swapping as a function of elevation). But there was still some uncertainty as to whether the astigmatism was in the main reflector surfaces or in the subreflector surfaces. The subreflector surfaces have been problematic in the past (Butler 1998), but the measuring machine measurements gave no indication that they were actually out of shape. This memo will describe an experiment I performed specifically to measure the astigmatism on the VLBA antennas, and to determine whether it is due to the main reflector surfaces or the subreflector surfaces.

Method

The method I chose was copied straight from one of the classic references on astigmatism in large radio telescopes: Cogdell & Davis 1973. In this paper, they describe a scheme to determine whether an antenna has astigmatism, and if so, how to determine the magnitude of the astigmatism. The method as in that paper is as follows:

1. Locate *a priori* focus.
2. Remove coma.
3. Locate the direction of maximum astigmatism. With the feed axially defocused from the maximum gain position, make a contour of the beam at the 3 or 10 dB level. If the beam is elliptical, astigmatism is possibly present. If defocusing on the opposite side of the maximum rotates the ellipse by 90°, then astigmatism is present.
4. Measure degree of astigmatism. Measure beamwidths in major and minor axis directions versus axial feed position. Data can then be compared with theoretical calculations to estimate astigmatism.

I assumed that items 1 and 2 above were already correctly done. The focus being exactly right wasn't particularly important, however, as I modified the scheme above slightly in order to account for some error in its setting. So, what I did was essentially step number 3 above.

Step number 4 could in theory be done, but I haven't attacked that problem to this point. My modified version of the scheme was as follows:

1. autolevel (at nominal focus)
2. set focus offset to -$2f$
3. take N random beam samples
4. set focus offset to -f
5. take N random beam samples
6. set focus offset to 0
7. take N random beam samples
8. set focus offset to +f
9. take N random beam samples
10. set focus offset to +$2f$
11. take N random beam samples
12. possibly change frequency and/or source
13. repeat steps 1-12

This was done at each of the VLBA antennas, in single dish pointing mode. This pattern was alternated between 1.3cm and 7mm. The reason for this alternation between wavelengths was to check whether the astigmatism was tied to the subreflector. Figure 1 shows a schematic of the layout of the feeds around the feed circle of the VLBA antennas. The K-band feed is 77° clockwise from the Q-band feed. Therefore, if the direction of the ellipticity of the beam at 1.3cm is 77° clockwise from the direction of the ellipticity of the beam at 7mm, then the astigmatism is almost certainly in the subreflector. If the direction of ellipticity of the beam was the same for both 1.3cm and 7mm, then the astigmatism is most likely in the main reflector. The sources chosen were strong H_2O and SiO masers. The H_2O masers chosen were W3OH and W49N, and both were strong enough to make relatively good beam maps. The SiO masers were RCas, UHer, and IKTau (SC only). RCas was by far the best of the three (much stronger), but UHer and IKTau also gave results which were usable. I used the same frequency setups which are used for the standard pointing runs. This implies that the SiO masers used an off-line IF to subtract out the background. I used both Stokes, averaging the results to increase SNR.

I chose values of $f = 2.8$mm and 5.4mm for the 7mm and 1.3cm wavelengths respectively. This was so that even if the *a priori* focus was quite bad, I should get samples of the beam on both sides of nominal focus.

The random beam samples were selected via Poisson selection with maximum radius equal to the first null in the primary beam pattern, in order to guarantee that the full extent of the primary lobe of the beam was sampled well. I chose a value of $N = 25$ for this run. The first sample taken in each sequence was constrained to be at the nominal beam center. The sampling was effected by inserting azimuth and elevation collimation offsets in the schedule files (`azcolim` and `elcolim` entries). I wanted to make the value of N small

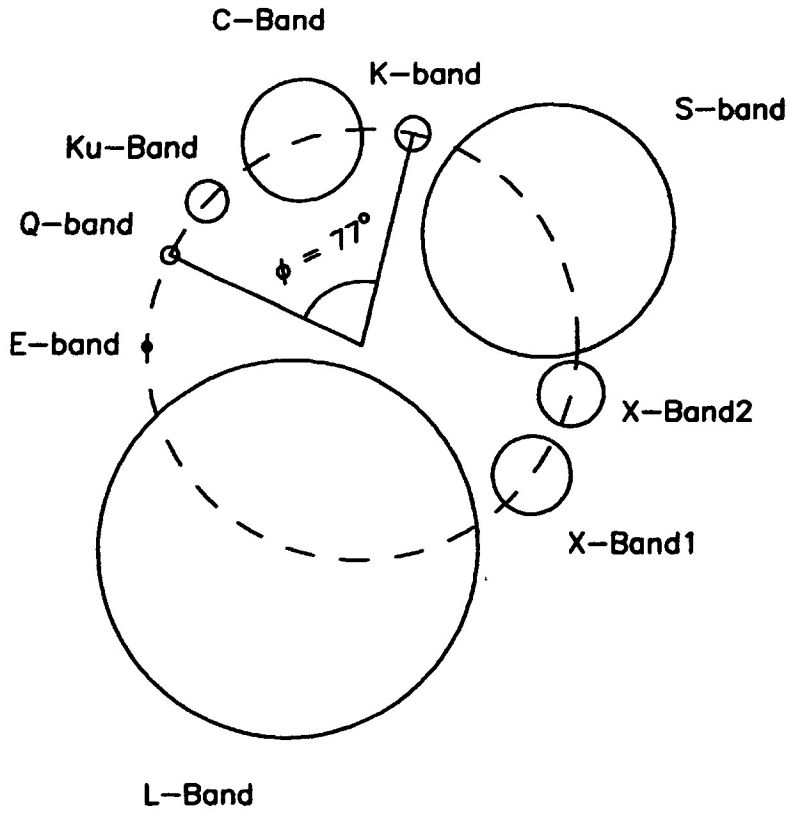

Figure 1: Layout of feeds around feed circle for VLBA antennas

enough that over the period taken for one complete cycle, the source would not move too far in elevation. This was because it was my initial intent to make beam maps at each elevation, and track how the ellipticity changed as a function of elevation. However, the SNR was not good enough, so only one (averaged over elevation) beam map was made at each antenna for each wavelength and each focus offset position. Given that I had to average all of the data, in any repeat of this experiment I would most likely increase N (maybe twice as big?).

All of the scheduling was done with a modified version of **sched** (it had to be modified to allow for more than 1000 sources), driven through a **perl** script. The script was run once for each station. A "control" file was written for each station - essentially just a ordered list of sources/wavelengths to be observed at that station. Output from the script was an "info" file, containing scan information for each station (source name, time, qualifier, and azimuth and elevation collimation offsets). Autoleveling was done at the beginning of each beam scan. Unfortunately, I did not sample the background baseline (off-source system temperature) for each beam in any way, which was a mistake, as it made normalization somewhat uncertain. This mistake should not be repeated in any future tests of this sort.

Weather

The experiment (TA023) was performed on June 3, 1998, from 0600 to 1700 UT. Weather was mostly clear in the southwest. OV had some strong winds. OV, BR, NL, and HN all had varying amounts of overcast and rain. This became clear in the analysis of the beam maps, as those locations with bad weather had marginal (at best) results.

Reduction

The raw power data was read from the monitor database via **sara**. The PWR records were written to a separate file for each antenna. After some hand editing (for data dropouts, etc...), an attempt at normalization was made. To do the normalization, I simply used the minimum sampled value as the off-source value. For the 7mm SiO maser sources this is not too bad, as the off-line spectral channels were first subtracted from the line-centered channels, doing much of the normalization in that preliminary step. For the 1.3cm H_2O maser sources, however, this could introduce some bias error into the beam maps. At the same time as the normalization was done, the "info" files created during the scheduling were used to add information on azimuth and elevation offset to each beam sample. The 1.3cm and 7mm data were also separated into individual files. The end result for each station and wavelength was a file containing a set of beam samples taken in the above described order of focus offset, where each beam sample had information on source, azimuth and elevation, azimuth and elevation offsets, and measured power in both RCP and LCP polarizations.

Each separate set of N samples of a beam (for each antenna, wavelength, source/elevation, and focus) was interpolated via Shepard interpolation (Renka 1988) and gridded onto a regular grid. These gridded data were then averaged together over elevation for each antenna, wavelength, and focus. The result was a beam map for each antenna at both 1.3cm and 7mm and at the 5 focus locations. These final maps were then fitted to find best fit ellipse parameters in the following way. The half-power point level was contoured for each beam map, using a modified variant of the **pgplot** contour-following routine **pgcont**. The (x,y) values for this contour were then fitted to find the best fit ellipse parameters: x_o, y_o (offset of center of ellipse); a (major axis length); b (minor axis length); and ψ (PA of major axis, counterclockwise from true north). The fitting algorithm used an algebraic distance minimizing technique (see Gander *et al.* 1994 - section 3.1). Note that I would have chosen a lower contour level, but some antennas/wavelengths/focus settings clearly suffered from sampling truncation effects, so this was not possible.

Results

Figures 2a-t show the resultant beam maps for all of the station/focus/wavelength combinations. Also shown on the figure for each station/wavelength is a table of derived ellipse parameters, and the fit major axis direction is indicated with a solid straight line on each beam map. Each station will now be discussed separately.

MK

Figures 2a and 2b show the results for MK for 1.3cm and 7mm. The antenna has quite well behaved beams at both wavelengths, even at the furthest focus throws. This is as expected, since measurements indicate that the MK antenna is one of the "better" VLBA antennas (Walker 1993). Even given the good behaviour of this antenna, however, it is clear that there is astigmatism present. At both wavelengths, the beam is elongated in directions which are nearly 90° apart on either side of nominal focus. There is also marginal evidence that the astigmatism is related to the subreflector, since for the two different wavelengths, the elongation directions are about 55° apart for similar focus settings.

BR

Figures 2c and 2d show the results for BR for 1.3cm and 7mm. It is clear that BR is a poor antenna for short wavelengths. This is also not unexpected, based on efficiency measurements (Walker 1993). In fact, of the antennas for which reliable results were obtained in this experiment, BR is by far the worst of the lot. Similar to MK, it is clear that astigmatism is present, and that it is related to the subreflector (for the same reasons). Weather was not particularly good at this site, so the experiment should be repeated to confirm the results.

OV

Figures 2e and 2f show the results for OV for 1.3cm and 7mm. OV seems to behave fairly well at 1.3cm, but at 7mm the beam deteriorates significantly at the furthest focus throws. However, recall that there was wind, overcast, and rain at this site, so the results should be considered only preliminary. The data seem to indicate subreflector related astigmatism, but any firm conclusion should await a repeat of the experiment in better weather.

KP

Figures 2g and 2h show the results for KP for 1.3cm and 7mm. Unfortunately, I messed up the scheduling for KP, and only 4 hours of data were obtained for this station. The beam maps are therefore of lower SNR than for the other antennas. Even given this smaller amount of data, it is clear that there is subreflector related astigmatism in the KP antenna.

PT

Figures 2i and 2j show the results for PT for 1.3cm and 7mm. PT is a fairly well behaved antenna, with serious degradation in the beams only at the furthest focus throws. However, there is still clear evidence of subreflector related astigmatism for this antenna.

LA

Figures 2k and 2l show the results for LA for 1.3cm and 7mm. These contours barely resemble a proper main beam, at either wavelength. I have inspected the data closely to

make sure that there is no particularly bad set of times which are corrupting the data, and indeed there is not. All of the individually sampled beams are this ratty. It is entirely unclear to me what is causing this to happen. Weather was good at LA, with clear skies, and relatively low temperatures and wind. Faced with these "beams", I find it impossible to draw any conclusions regarding astigmatism in this antenna. Obviously, the experiment should be repeated for this site.

FD

Figures 2m and 2n show the results for FD for 1.3cm and 7mm. The beams are good except at the $-2f$ focus position (due to a slightly incorrect focus setting?). However, there is still clear evidence of subreflector related astigmatism for this antenna.

NL

Figures 2o and 2p show the results for NL for 1.3cm and 7mm. The bad weather is readily apparent in the 1.3cm beam maps. The 7mm beam maps are much better, perhaps because of the decreased sensitivity to atmospheric water, or possibly because of the off-line subtraction. The 7mm results seem to indicate astigmatism, but it is hard to tell if it is related to the subreflector given the poor quality 1.3cm data. The experiment needs to be repeated for this site.

HN

Figures 2q and 2r show the results for HN for 1.3cm and 7mm. This station has very similar results as NL, in that the bad weather is readily apparent in the 1.3cm beam maps, yet the 7mm beam maps are much better. Similar to NL, the 7mm results seem to indicate astigmatism, but it is hard to tell if it is related to the subreflector given the poor quality 1.3cm data. The experiment needs to be repeated for this site.

SC

Figures 2s and 2t show the results for SC for 1.3cm and 7mm. Behaviour is fairly good with the exception of the $-2f$ focus position (due to a slightly incorrect focus setting?). There is clear evidence of subreflector related astigmatism.

Summary

Table 1 shows the results for the different stations/wavelengths. Note that LA is excluded, based on the poor beam maps for that station. In this table, ψ_o is the major axis angle at negative focus offset, $\Delta\psi$ is the difference between ψ_o and the major axis angle at positive focus offset (the two focus settings used are also indicated in that column), and BWB is a crude measure of the BeamWidth Broadening. The BWB is estimated via: BWB $= (a-b)/a$, averaged over two focus locations which are approximately adjacent to what appears to be

the nominal focus position (the two focus settings used are indicated in that column). This is only a crude estimate, but gives guidance as to the amount of astigmatism at each station.

Table 1: Summary of astigmatism data

station	wavelength	ψ_o	$\Delta\psi$	BWB[a]
MK	1.3cm	-64	79 $(-2f,+2f)$	0.068 $(-2f,0)$
MK	7mm	+63	84 $(-2f,+2f)$	0.12 $(none,0)$
BR	1.3cm	-29	85 $(-f,+f)$	0.23 $(-f,+f)$
BR	7mm	+63	76 $(-f,+f)$	0.32 $(-f,+f)$
OV	1.3cm	-19	55 $(-f,+2f)$	0.11 $(-2f,+f)$
OV	7mm	+63	84 $(-2f,+2f)$	0.17 $(-2f,0)$
KP	1.3cm	-27	102 $(-2f,+2f)$	0.11 $(-f,+f)$
KP	7mm	+49	87 $(-2f,+2f)$	0.14 $(-f,+f)$
PT	1.3cm	+25	95 $(-2f,+2f)$	0.072 $(-f,+f)$
PT	7mm	-37	74 $(-f,+f)$	0.089 $(-f,+f)$
FD	1.3cm	+24	107 $(-f,+2f)$	0.078 $(0,+2f)$
FD	7mm	-62	75 $(-f,+2f)$	0.14 $(0,+2f)$
NL[b]	1.3cm	-56	88 $(-f,+f)$	0.27 $(-f,+f)$
NL	7mm	-14	80 $(-f,+f)$	0.073 $(-f,+f)$
HN[b]	1.3cm	-84	76 $(-f,+f)$	0.076 $(-f,+f)$
HN	7mm	+58	79 $(-2f,+f)$	0.15 $(-2f,+f)$
SC	1.3cm	+16	51 $(-f,+2f)$	0.11 $(0,+2f)$
SC	7mm	+76	61 $(-f,+2f)$	0.19 $(-f,+f)$

[a] BWB $= (a-b)/a$ averaged for the two indicated focus positions

[b] Results badly affected by weather

Investigation of Table 1 clearly shows astigmatism for all antennas except LA (because of problems discussed above). For these antennas, the value of $\Delta\psi$ is nearly 90° for both wavelengths. The mean value of $\Delta\psi$ in Table 1 (NL and HN 1.3cm values excluded) is $\sim 80°$.

Table 2 shows values of the difference between the values of ψ_o for the two wavelengths for those antennas with relatively good data at both wavelengths (LA, NL, and HN excluded). The angle ϕ is the clockwise angle from the major axis position at 7mm (ψ_o) to that at 1.3cm. BR, OV, KP, FD, and SC all have values of ϕ close enough to 77° to indicate subreflector related astigmatism. For MK and PT, the angles are nearly 180 degrees away from the angle which would indicate subreflector related astigmatism. For MK, I think this is just because the antenna is so well behaved that the angle of beam ellipticity is hard to measure at K-band. I don't know how to explain the PT result. The beam ellipticities are relatively large and easy to measure for that antenna. It just seems like the rotational direction has been reversed. Also note that for most of the antennas, the axis of symmetry of the subreflector seems to play some role in the astigmatism. This is indicated by the fact that the values of ψ_o are near the angles of the Q-band and K-band feeds (the Q-band feed sits at +65°, K-band at -12°). This is true for MK (7mm), BR (both), OV (both), KP (both), HN (7mm), and SC (7mm).

Table 2: Subreflector astigmatism indicator

station	ϕ
MK	127
BR	92
OV	82
KP	76
PT	118
FD	94
SC	60

Pointing

A byproduct of this experiment is an estimate of the pointing errors for each antenna. For each separate beam map, the max in the interpolated map is taken as the pointing center, and from that, a pointing offset is determined. The mean of the pointing offset numbers is then an estimate of the average blind pointing offset for the antenna. Table 3 shows these numbers (along with the rms) for all of the antennas except LA. These numbers are a weighted average of the values for 1.3cm and 7mm for each antenna. Note that the values for antennas which had marginal weather (BR, OV, NL, and HN) should of course be regarded as only very rough estimates.

Table 3: Pointing offsets at VLBA antennas during astigmatism run

station	pointing offset (arcsec)
MK	8.3 ± 3.9
BR	12.1 ± 5.2
OV	11.1 ± 5.2
KP	6.7 ± 3.1
PT	8.3 ± 3.6
FD	8.8 ± 4.1
NL	10.6 ± 4.8
HN	10.0 ± 4.5
SC	9.5 ± 4.1

Conclusions

All antennas except LA (very poor data) clearly show the symptoms of astigmatism. For the antennas which have good data at both 1.3cm and 7mm (HN, NL, and LA excepted), all but PT and MK have indications that the astigmatism is related to the subreflector (and probably related to the actual axis of symmetry of the subreflector). The lack of such a signature for MK is probably simply due to the inability to accurately measure the K-band beam ellipticity. The lack of such a signature for PT is somewhat confusing, since it is clear that the angles of beam elongation are different for 1.3cm and 7mm, yet the specific directions are not right for subreflector related astigmatism. BR is by far the worst of the antennas in

terms of astigmatism. MK is the best. This type of experiment needs to be repeated again, with some minor modifications to the procedure (more beam samples per cycle, good zero level measurement, sample further out in the beam, etc...). It would probably be best to do it in winter, to try to catch good weather at most of the sites.

References

Butler, B., Options for VLBA Antenna Surface Measurement, VLBA Test Memo No. 57, 1998

Cogdell, J.R., & J.H. Davis, Astigmatism in Reflector Antennas, *IEEE Trans. Ant. Prop., AP-21*, 565–567, 1973

Gander, W., G.H. Golub, & R. Strebel, Least-Squares Fitting of Circles and Ellipses, *BIT, 34*, 558–578, 1994

Renka, R.J., Multivariate Interpolation of Large Sets of Scattered Data, *ACM Trans. Math. Soft., 14*, 139–148, 1988

Walker, C., VLBA System Temperatures and Efficiencies, VLBA Test Memo No. 46, 1993

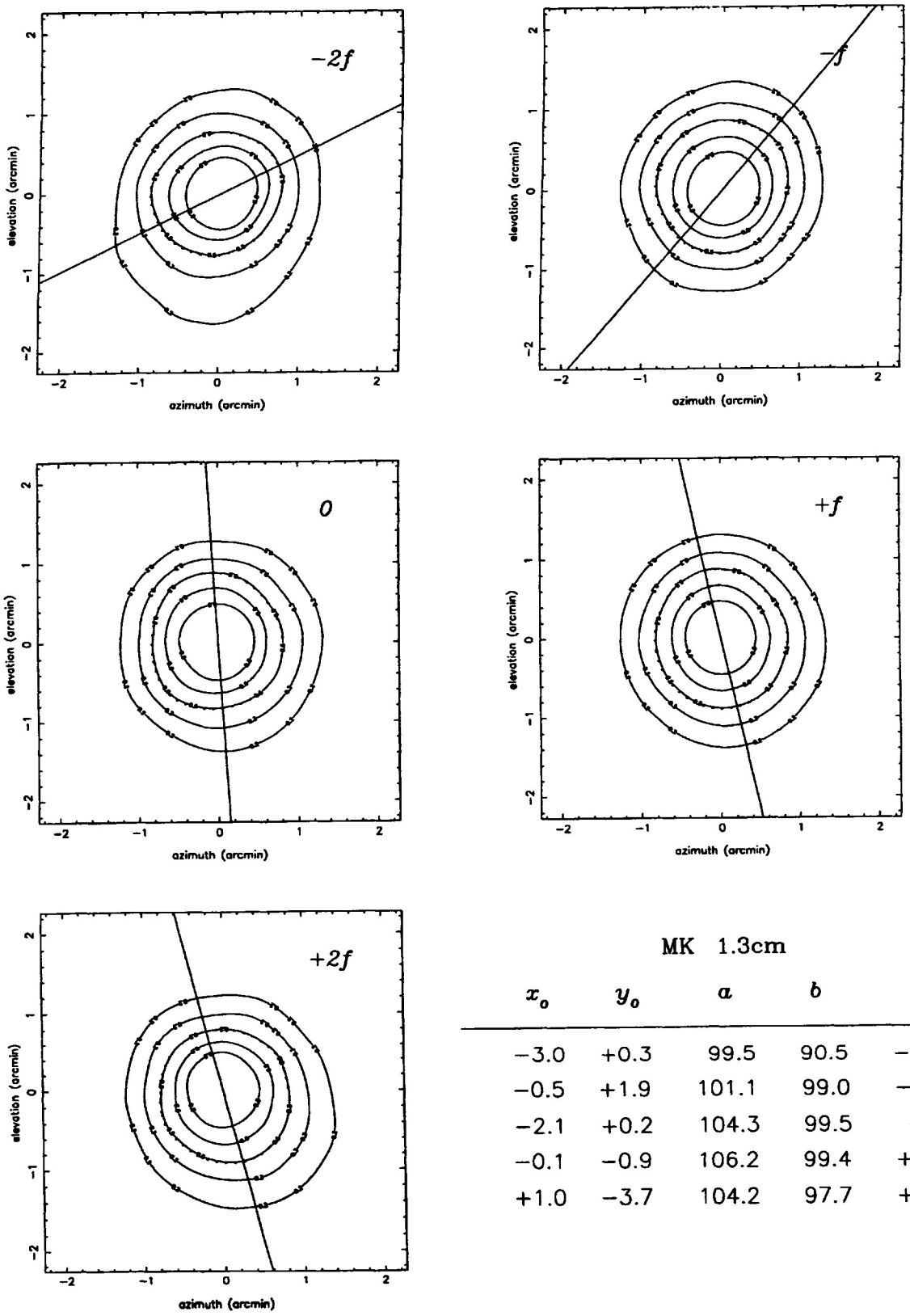

MK 1.3cm

x_o	y_o	a	b	ψ
−3.0	+0.3	99.5	90.5	−64.0
−0.5	+1.9	101.1	99.0	−40.3
−2.1	+0.2	104.3	99.5	+3.6
−0.1	−0.9	106.2	99.4	+12.9
+1.0	−3.7	104.2	97.7	+14.6

Figure 2b: Beam maps for MK at 1.3 cm.

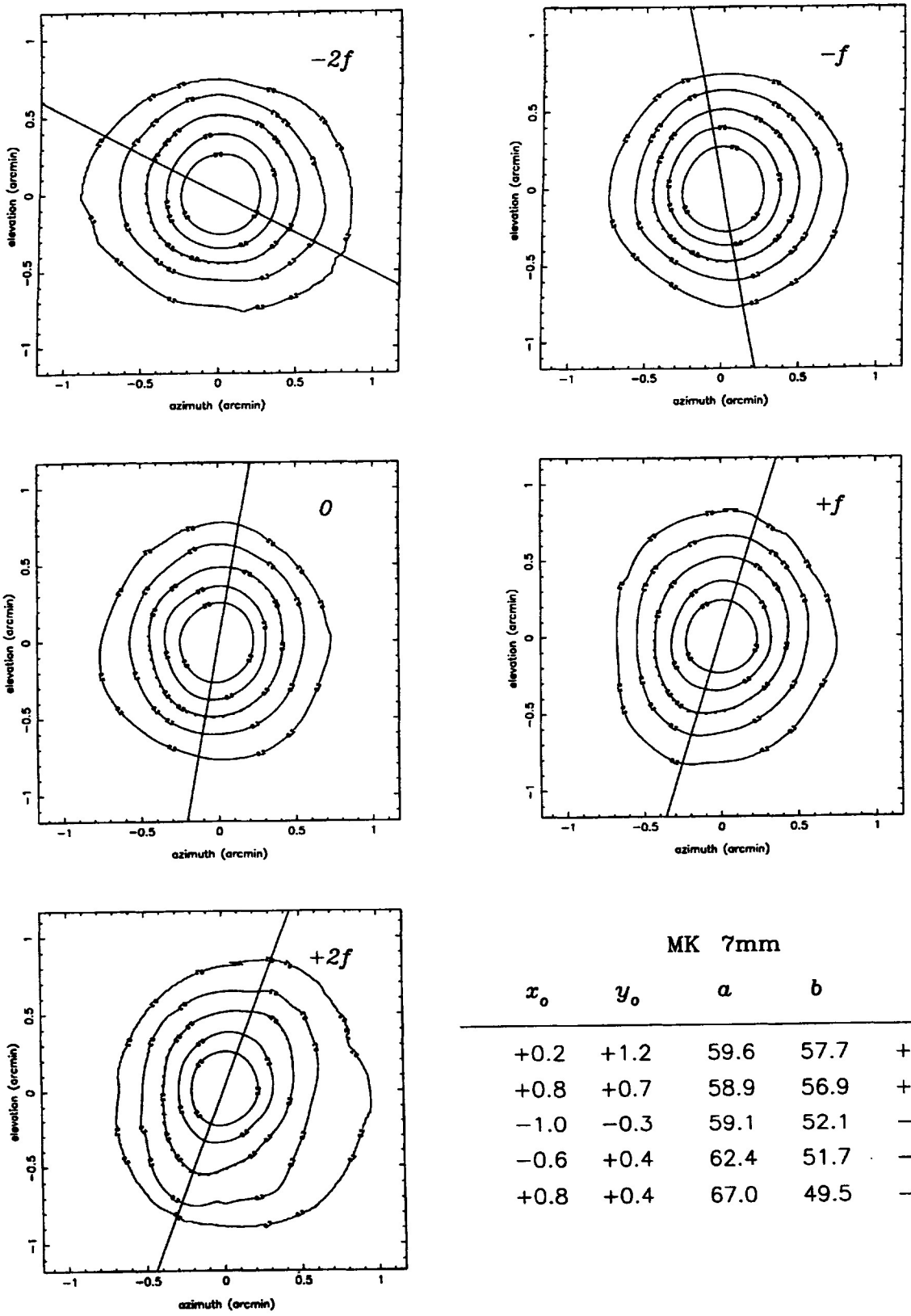

MK 7mm

x_o	y_o	a	b	ψ
+0.2	+1.2	59.6	57.7	+62.9
+0.8	+0.7	58.9	56.9	+10.7
−1.0	−0.3	59.1	52.1	−10.1
−0.6	+0.4	62.4	51.7	−17.2
+0.8	+0.4	67.0	49.5	−20.6

Figure 2c: Beam maps for MK at 7 mm.

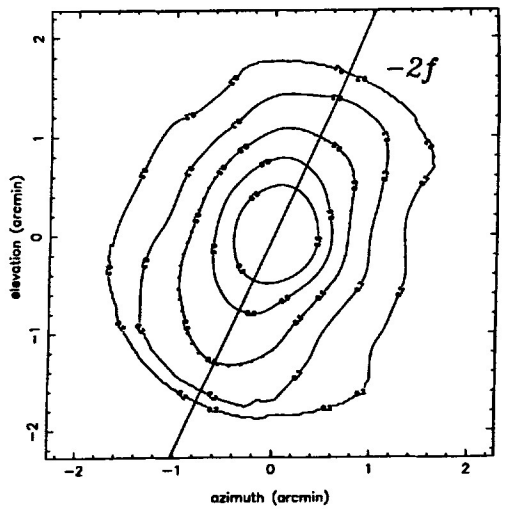

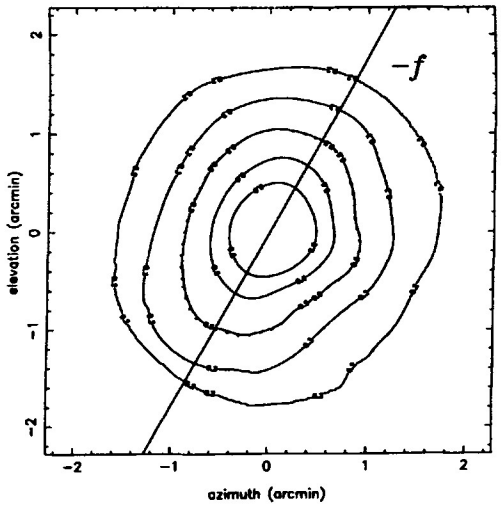

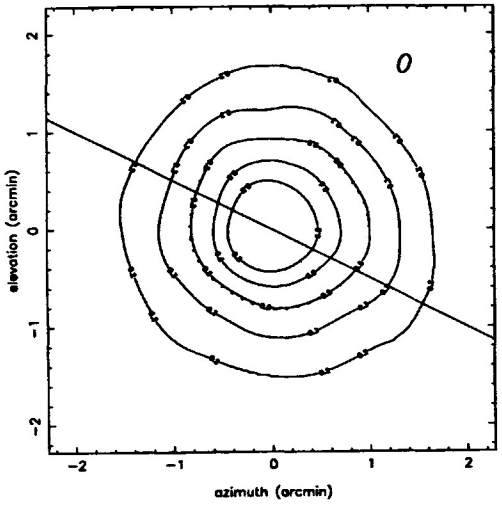

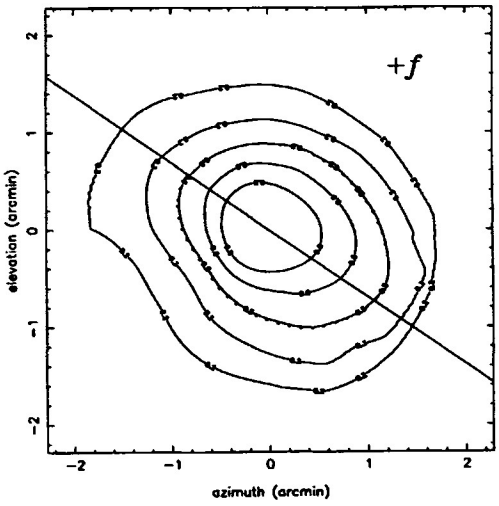

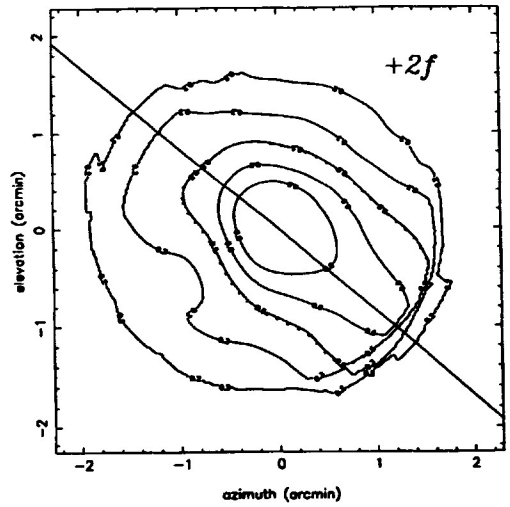

BR 1.3cm

x_o	y_o	a	b	ψ
−5.9	−6.1	153.2	92.9	−24.3
−1.5	−0.5	130.7	102.5	−29.2
+4.1	+3.6	111.2	103.7	+63.4
+9.1	−3.5	136.4	102.1	+55.4
+18.5	−11.3	166.4	99.2	+49.8

Figure 2d: Beam maps for BR at 1.3 cm.

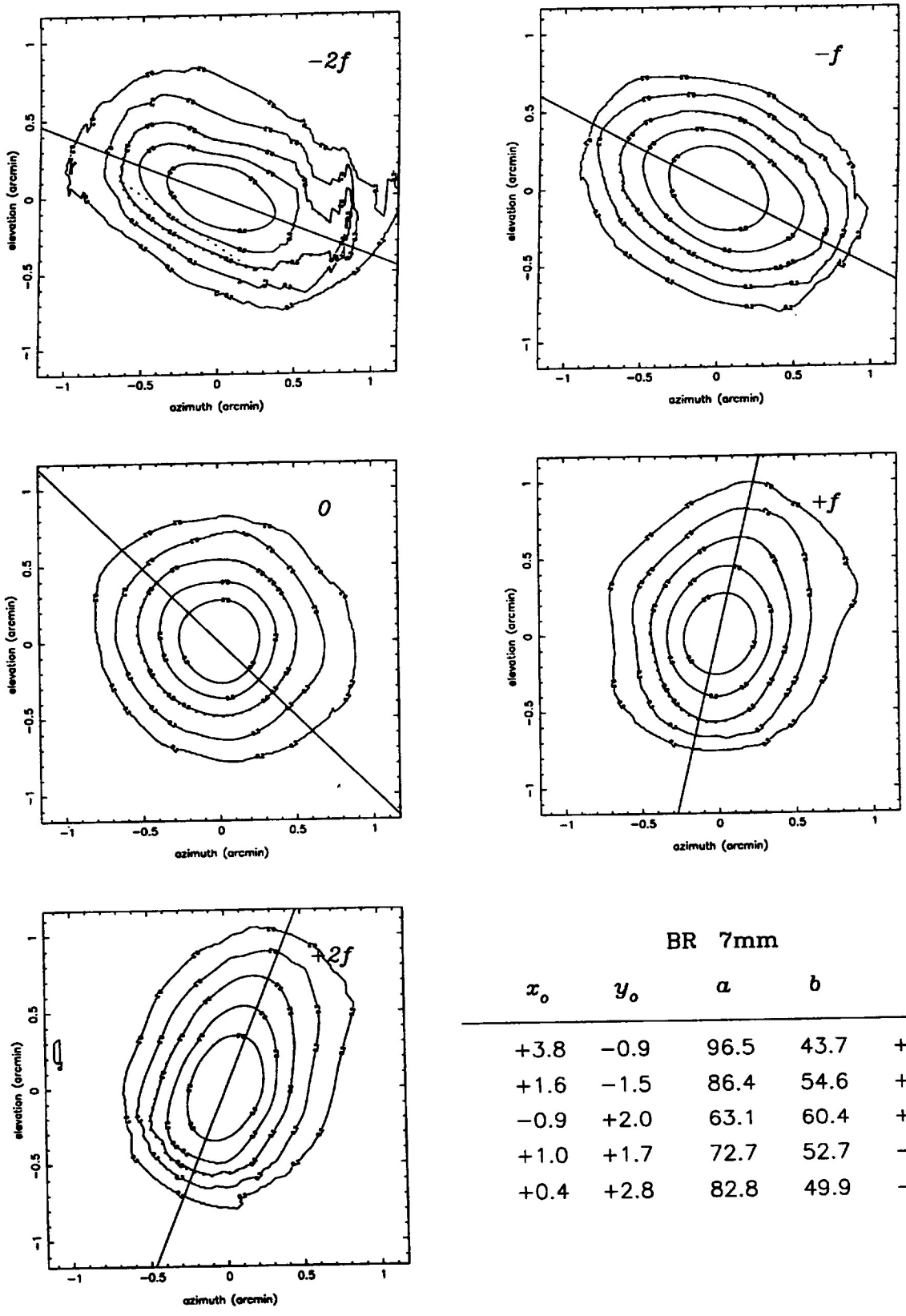

BR 7mm

x_o	y_o	a	b	ψ
+3.8	−0.9	96.5	43.7	+68.4
+1.6	−1.5	86.4	54.6	+62.7
−0.9	+2.0	63.1	60.4	+45.7
+1.0	+1.7	72.7	52.7	−13.2
+0.4	+2.8	82.8	49.9	−22.0

Figure 2e: Beam maps for BR at 7 mm.

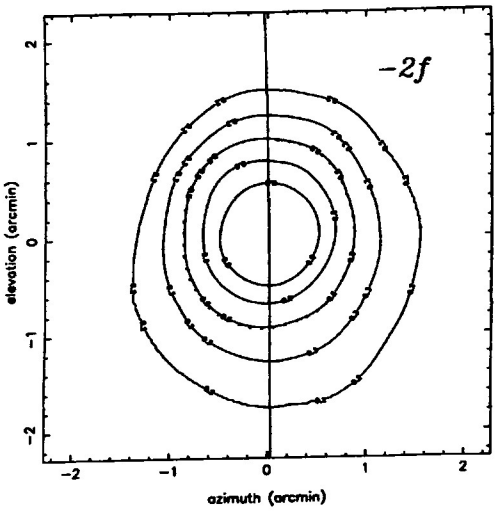

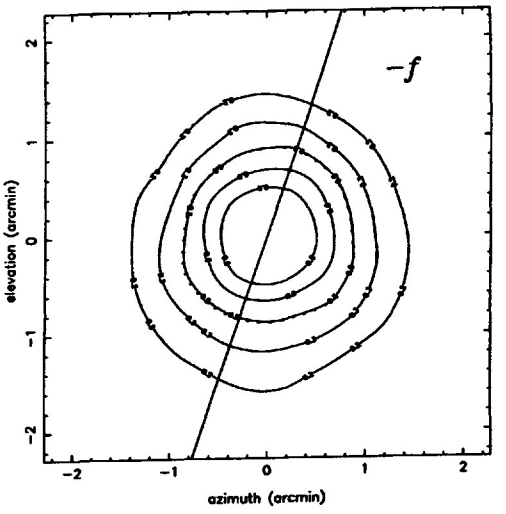

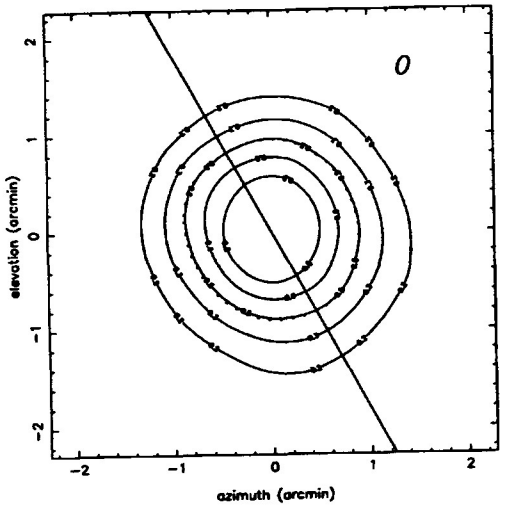

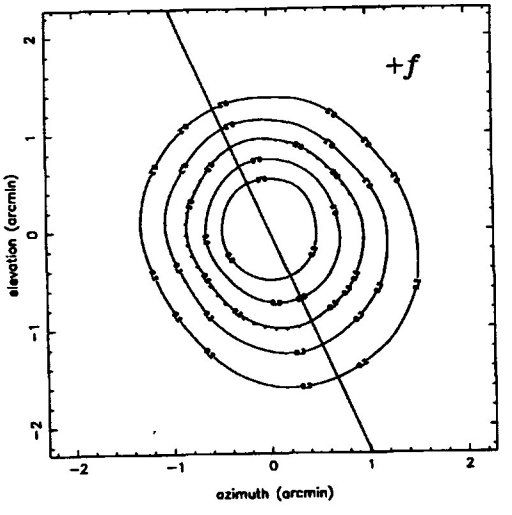

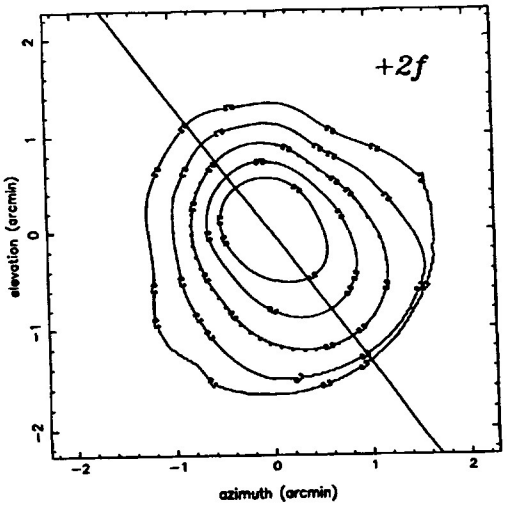

OV 1.3cm

x_o	y_o	a	b	ψ
−1.1	+2.1	118.0	106.1	+0.9
+0.6	−0.9	107.8	106.5	−18.7
+0.5	+1.2	113.1	104.4	+28.7
+2.9	−1.9	118.0	104.5	+24.1
+9.4	−11.3	138.5	105.6	+36.7

Figure 2f: Beam maps for OV at 1.3 cm.

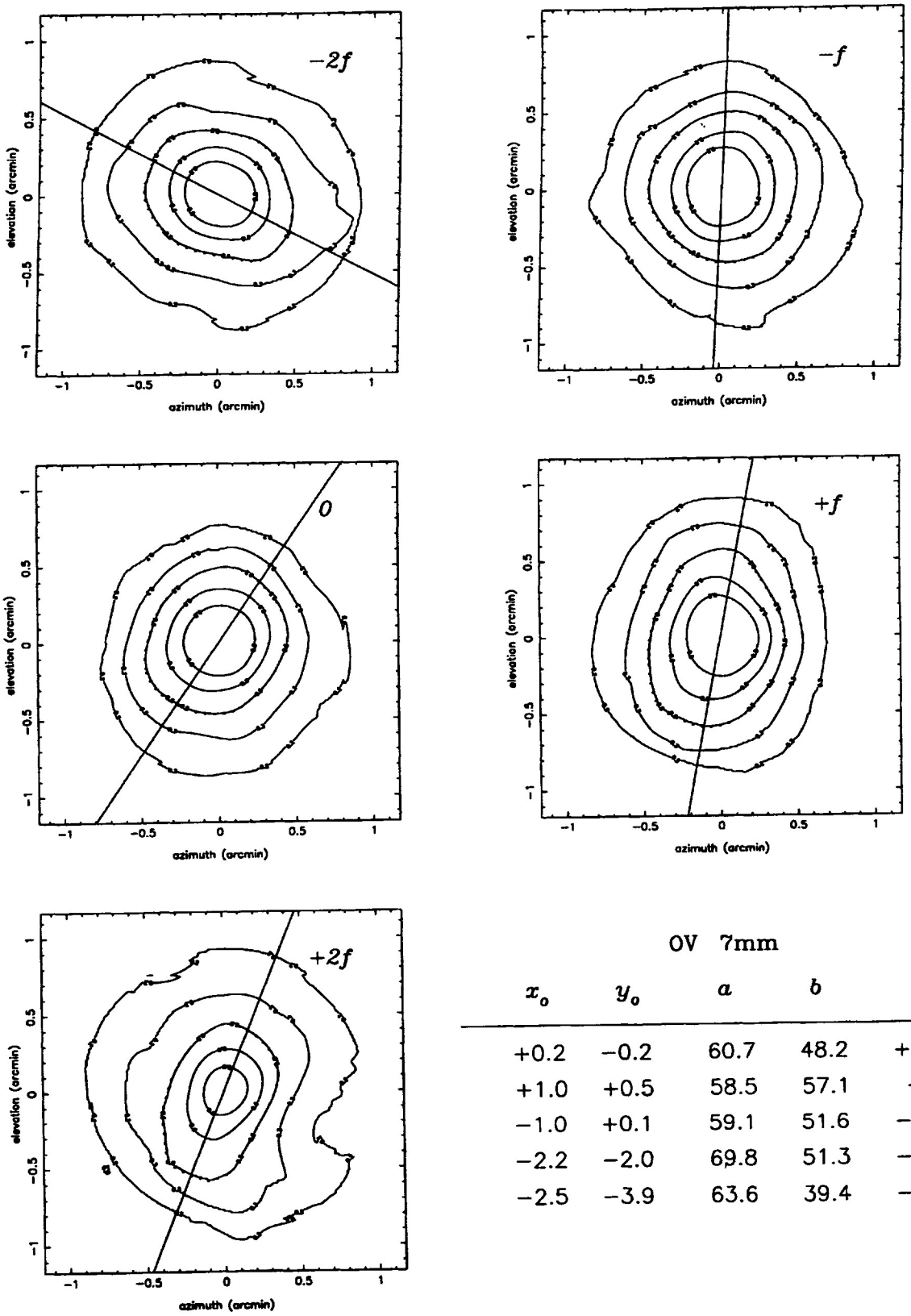

OV 7mm

x_o	y_o	a	b	ψ
+0.2	−0.2	60.7	48.2	+62.5
+1.0	+0.5	58.5	57.1	−1.8
−1.0	+0.1	59.1	51.6	−34.4
−2.2	−2.0	69.8	51.3	−10.7
−2.5	−3.9	63.6	39.4	−21.9

Figure 2g: Beam maps for OV at 7 mm.

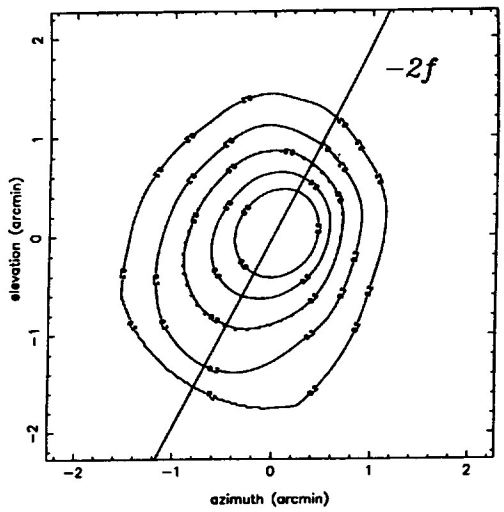

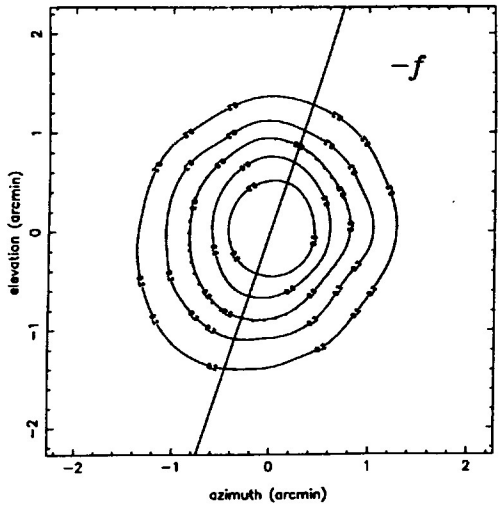

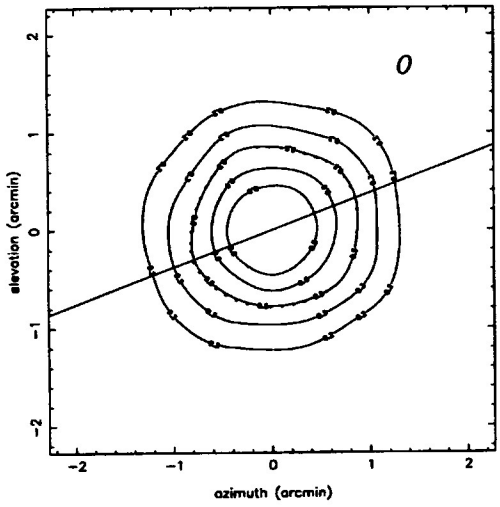

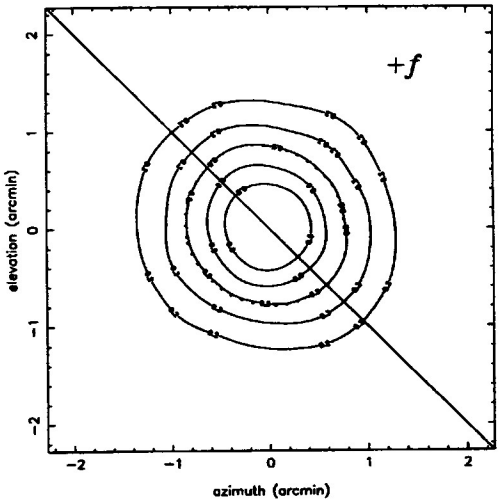

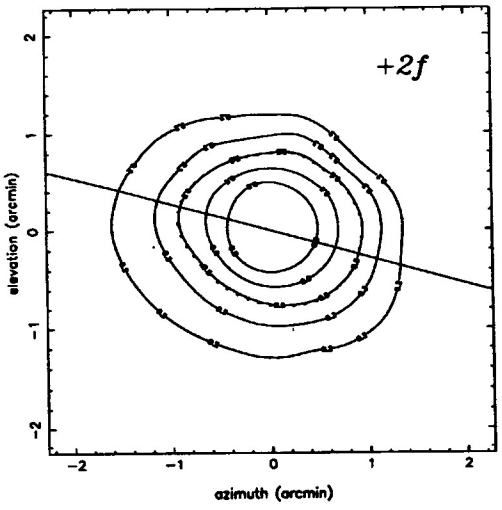

KP 1.3cm

x_o	y_o	a	b	ψ
−6.7	−3.5	112.2	90.6	−27.3
−3.1	+0.5	110.1	96.1	−18.3
+2.0	+1.2	103.7	99.4	−69.2
−2.3	+1.4	103.4	94.7	+44.9
+1.8	+1.2	112.0	92.6	+74.8

Figure 2h: Beam maps for KP at 1.3 cm.

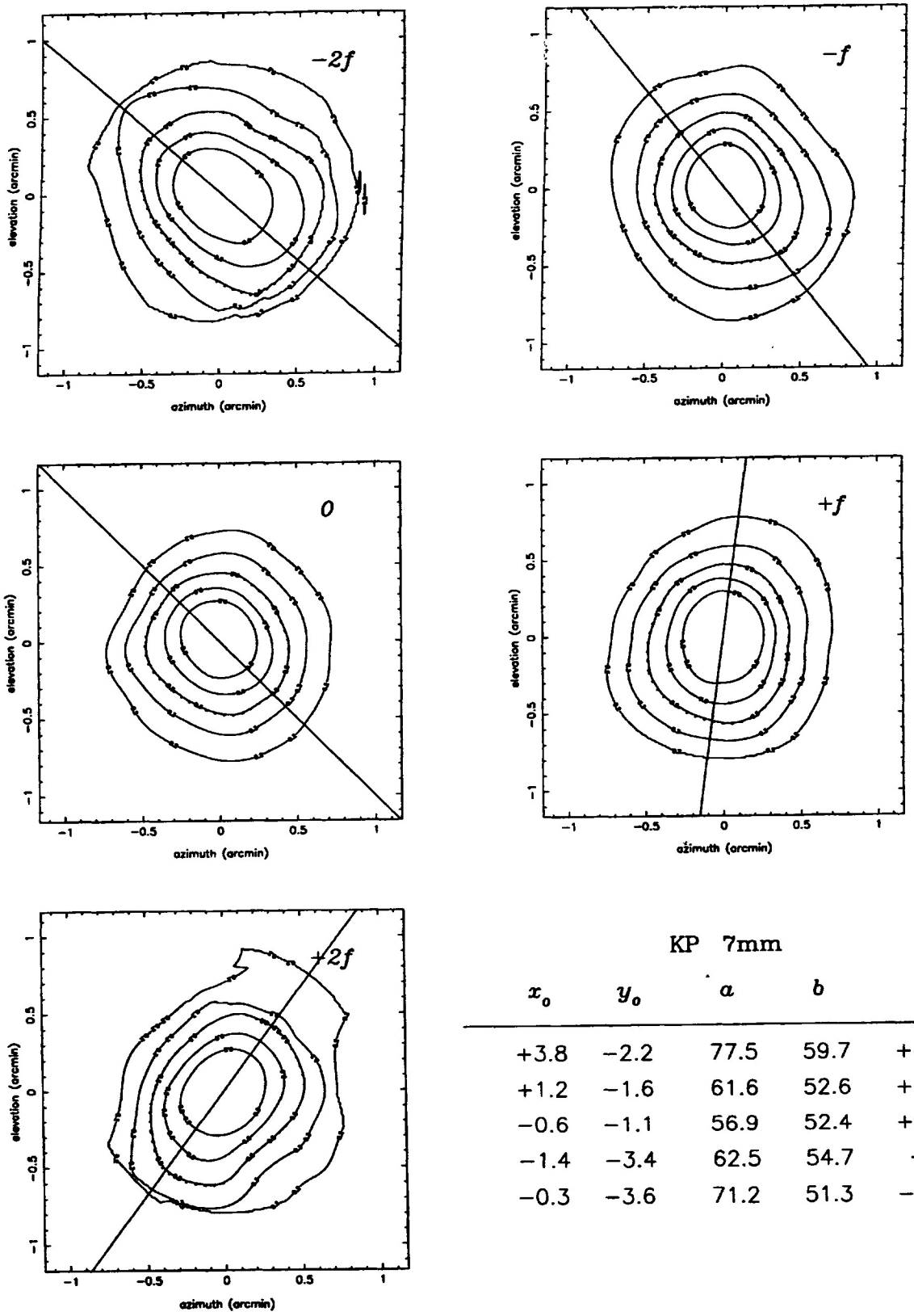

KP 7mm

x_o	y_o	a	b	ψ
+3.8	−2.2	77.5	59.7	+49.3
+1.2	−1.6	61.6	52.6	+39.0
−0.6	−1.1	56.9	52.4	+44.8
−1.4	−3.4	62.5	54.7	−7.6
−0.3	−3.6	71.2	51.3	−36.6

Figure 2i: Beam maps for KP at 7 mm.

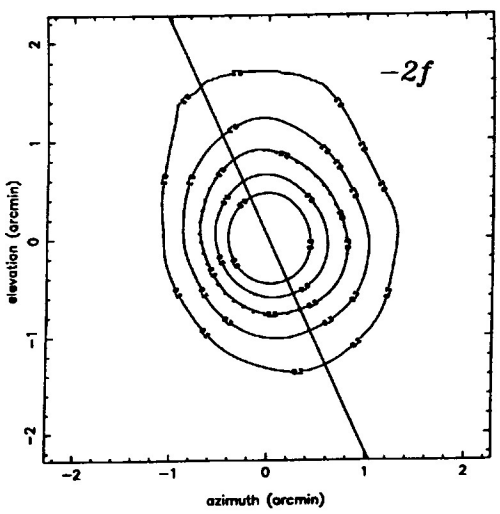

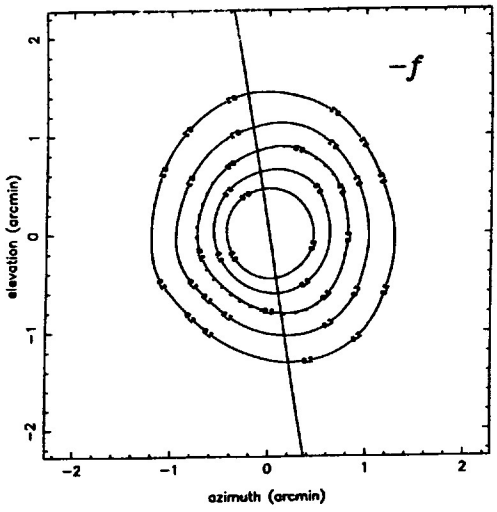

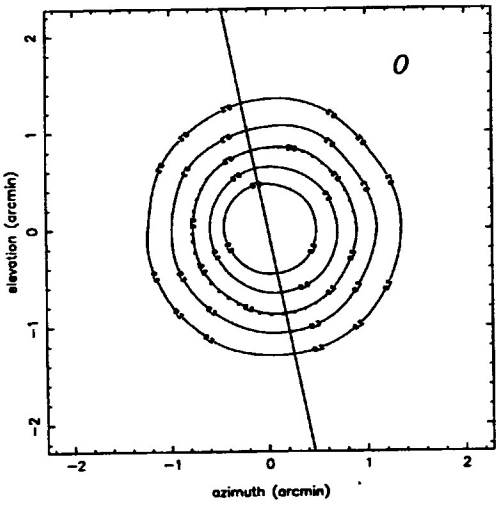

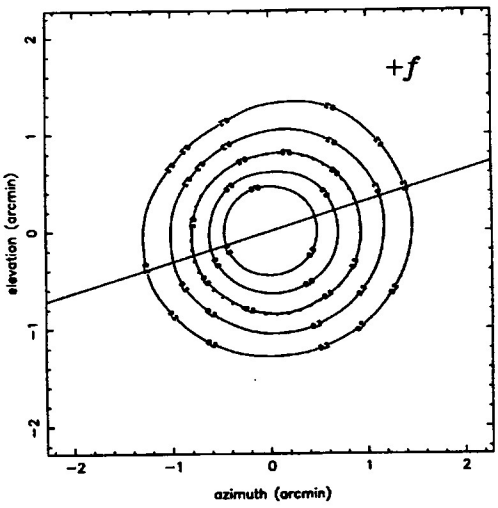

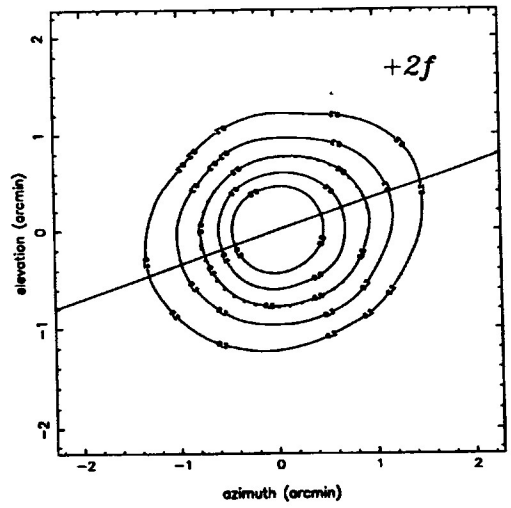

PT 1.3cm

x_o	y_o	a	b	ψ
+1.7	+2.1	103.2	86.9	+24.5
+3.1	+1.5	102.2	93.5	+9.1
+3.1	−0.9	103.8	100.2	+11.5
+3.7	−1.5	105.5	99.3	−72.6
+4.1	−0.2	105.0	92.7	−70.8

Figure 2j: Beam maps for PT at 1.3 cm.

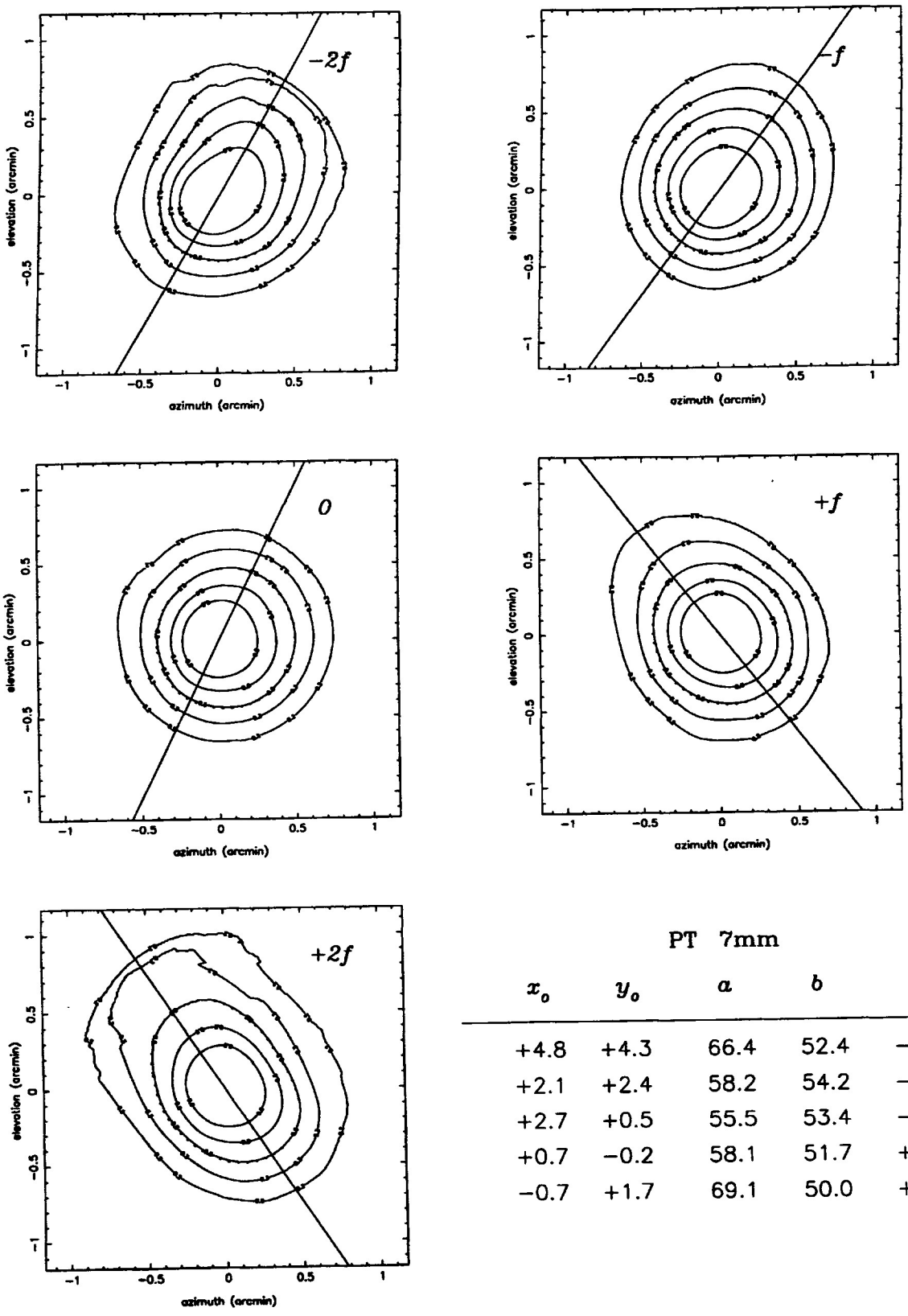

PT 7mm

x_o	y_o	a	b	ψ
+4.8	+4.3	66.4	52.4	−29.5
+2.1	+2.4	58.2	54.2	−36.1
+2.7	+0.5	55.5	53.4	−26.0
+0.7	−0.2	58.1	51.7	+37.9
−0.7	+1.7	69.1	50.0	+33.8

Figure 2k: Beam maps for PT at 7 mm.

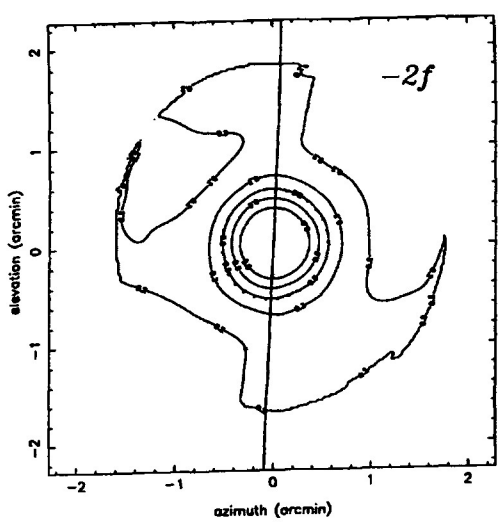

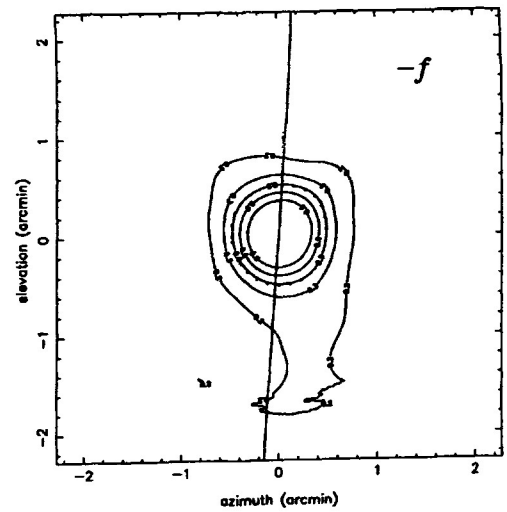

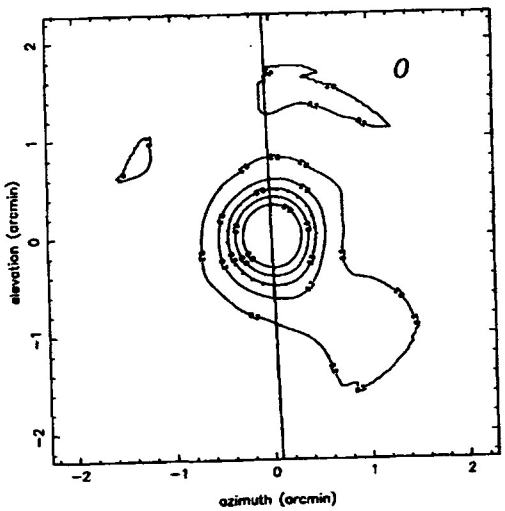

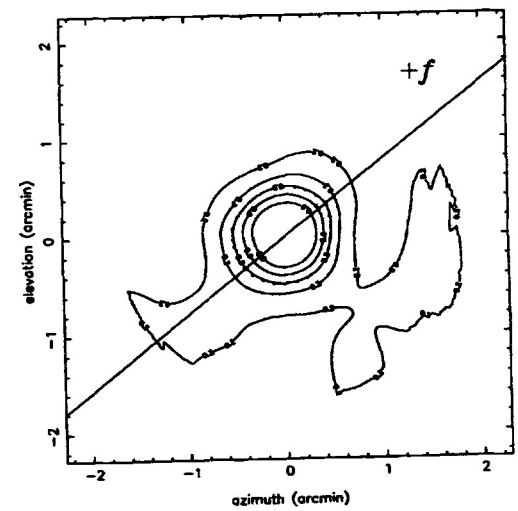

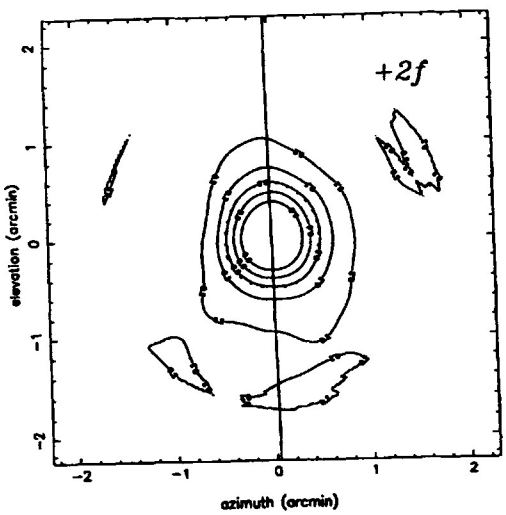

LA 1.3cm

x_o	y_o	a	b	ψ
+0.4	+0.7	66.5	65.5	−2.4
+0.2	+1.0	61.8	59.0	−3.8
+0.1	−0.9	59.6	54.5	+1.7
−1.3	+0.5	62.6	58.6	−51.8
+0.4	+1.4	65.5	58.3	+0.9

Figure 2l: Beam maps for LA at 1.3 cm.

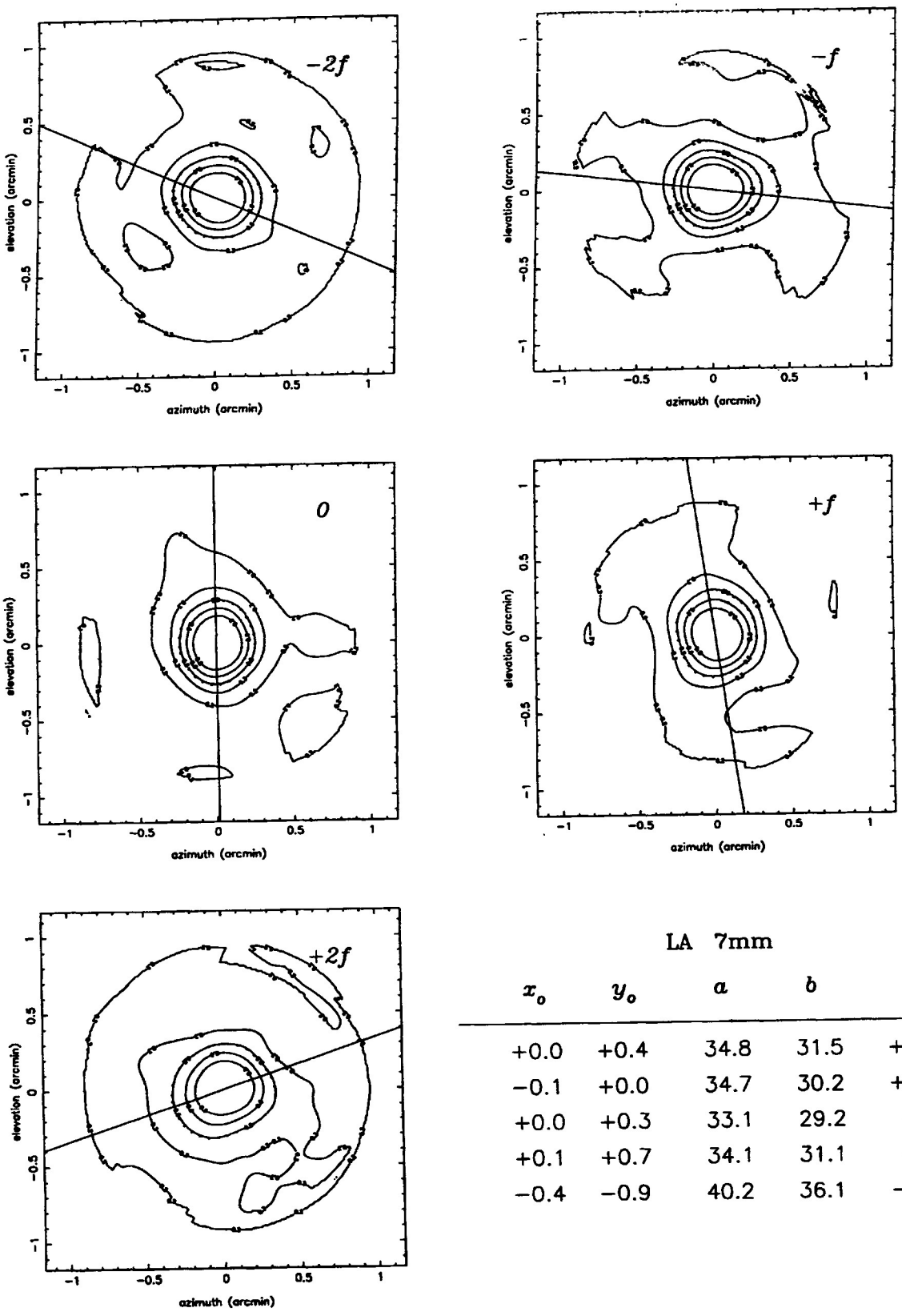

LA 7mm

x_o	y_o	a	b	ψ
+0.0	+0.4	34.8	31.5	+66.9
−0.1	+0.0	34.7	30.2	+83.3
+0.0	+0.3	33.1	29.2	+0.5
+0.1	+0.7	34.1	31.1	+8.6
−0.4	−0.9	40.2	36.1	−71.3

Figure 2m: Beam maps for LA at 7 mm.

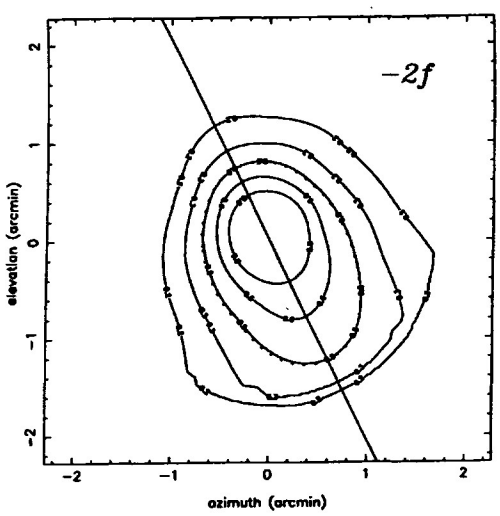

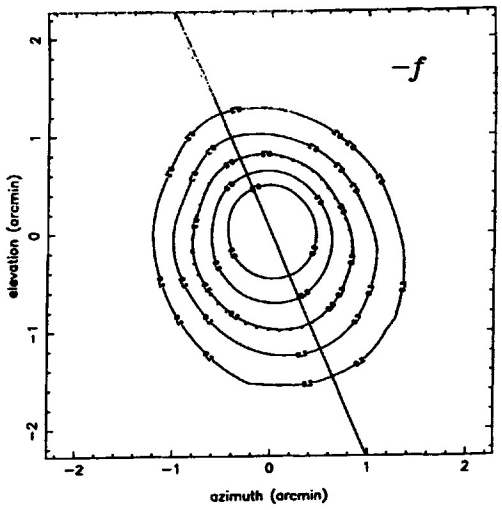

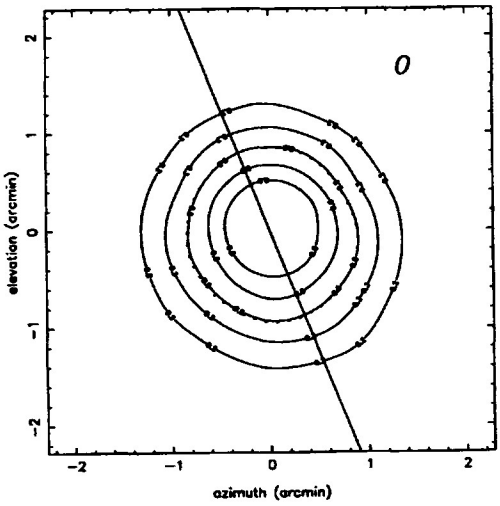

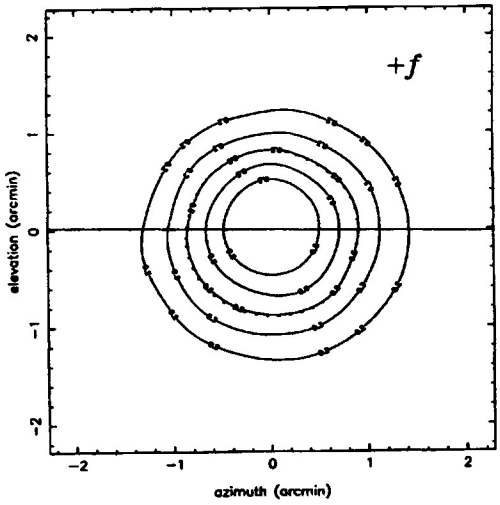

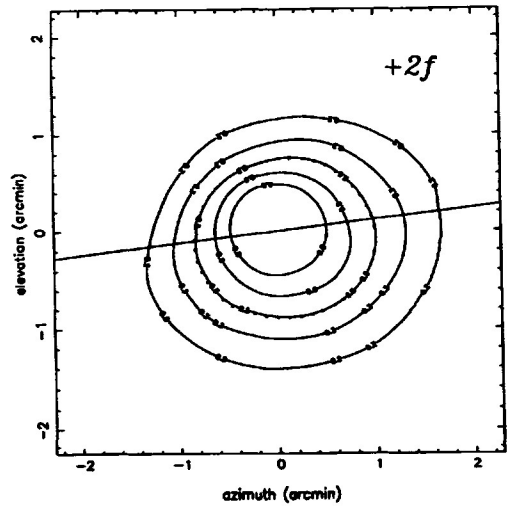

FD 1.3cm

x_o	y_o	a	b	ψ
+7.6	−13.9	132.4	86.4	+26.0
−0.3	−6.1	110.2	95.9	+23.5
+1.2	−2.8	107.8	102.1	+21.7
+0.7	−2.9	106.2	102.5	+89.4
+4.5	−4.9	110.4	99.1	−83.2

Figure 2n: Beam maps for FD at 1.3 cm.

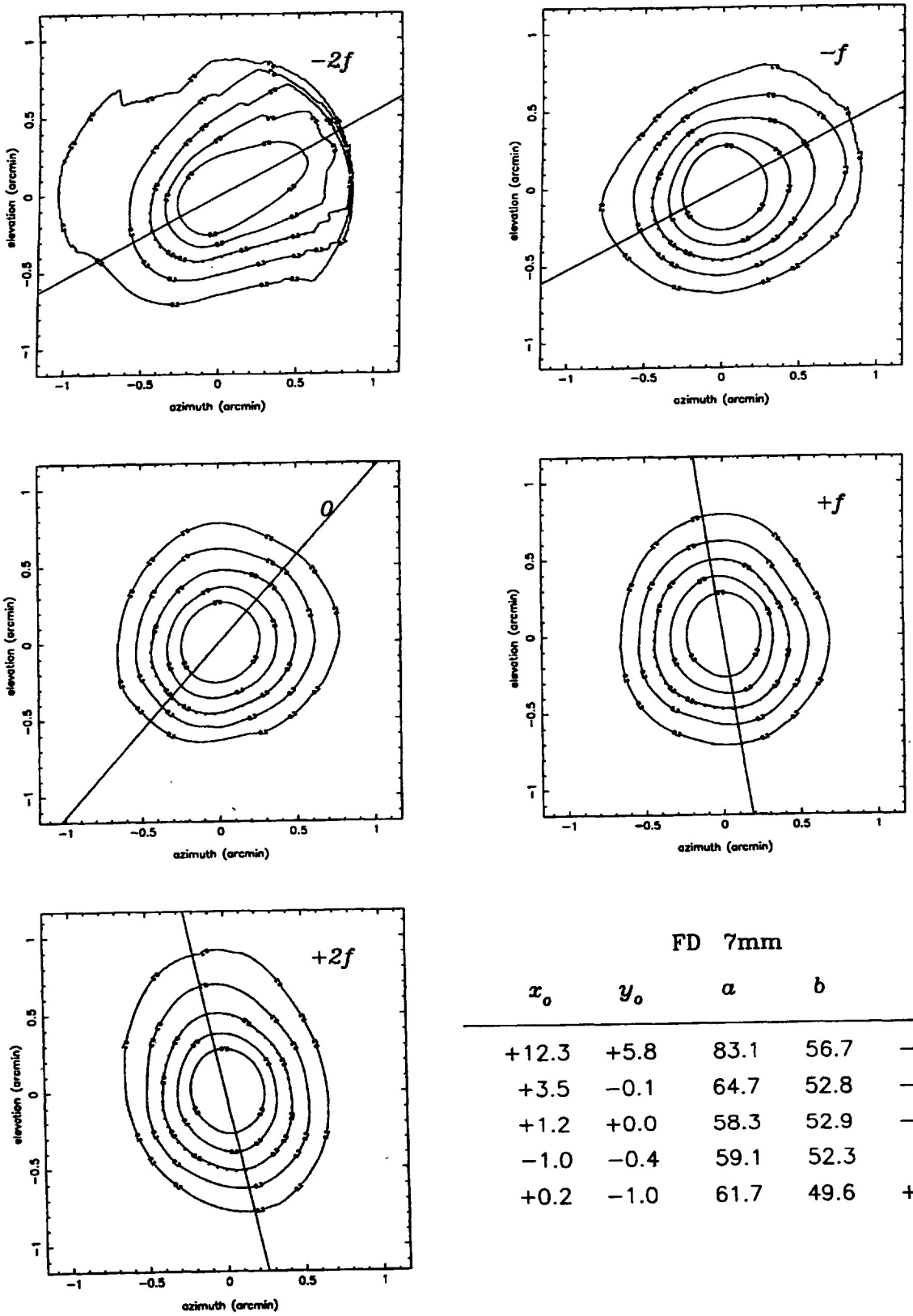

FD 7mm

x_o	y_o	a	b	ψ
+12.3	+5.8	83.1	56.7	−61.7
+3.5	−0.1	64.7	52.8	−62.4
+1.2	+0.0	58.3	52.9	−41.4
−1.0	−0.4	59.1	52.3	+9.1
+0.2	−1.0	61.7	49.6	+12.4

Figure 2o: Beam maps for FD at 7 mm.

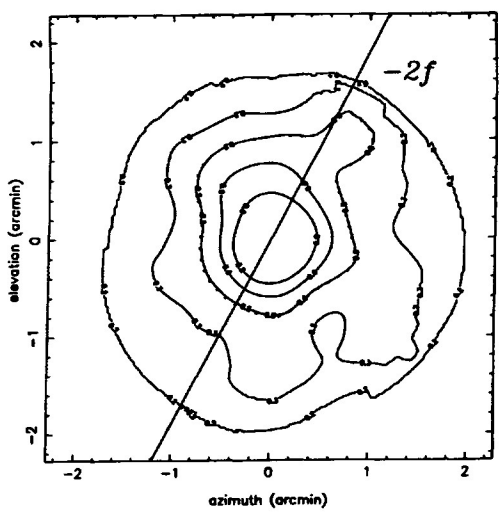

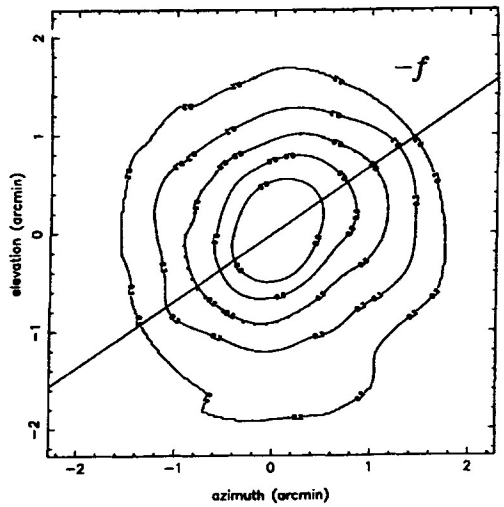

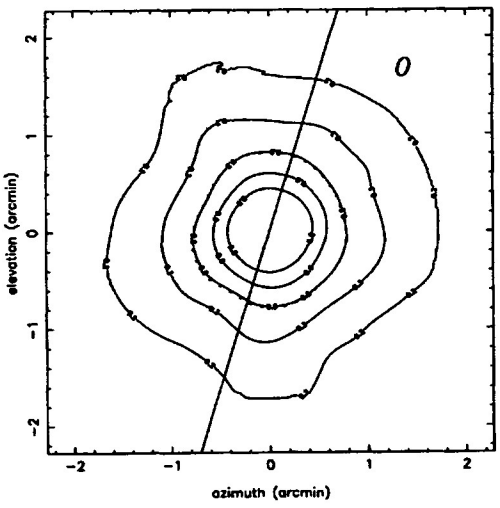

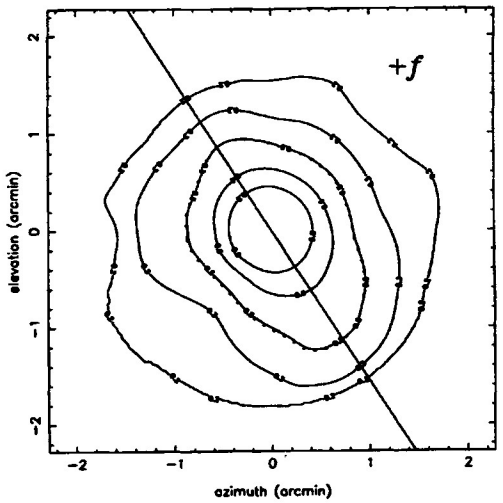

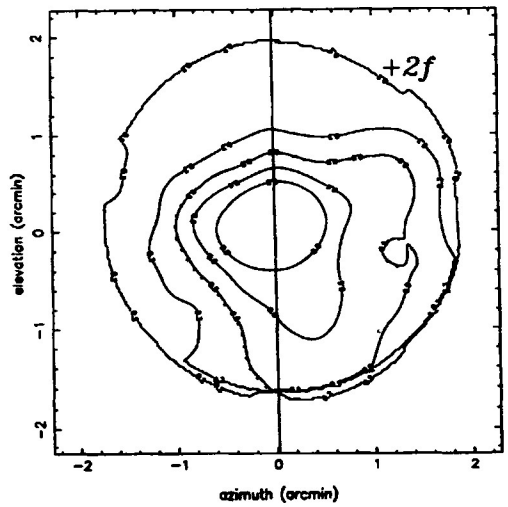

NL 1.3cm

x_o	y_o	a	b	ψ
+4.9	+15.3	126.4	96.0	−27.7
+5.5	+3.6	131.2	103.2	−55.6
+0.3	+0.7	95.0	91.3	−17.2
+4.3	−6.7	139.6	93.7	+32.8
+15.8	−16.9	149.7	135.4	+0.5

Figure 2p: Beam maps for NL at 1.3 cm.

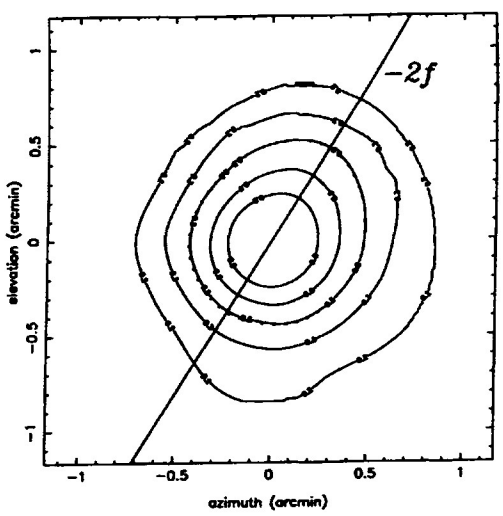

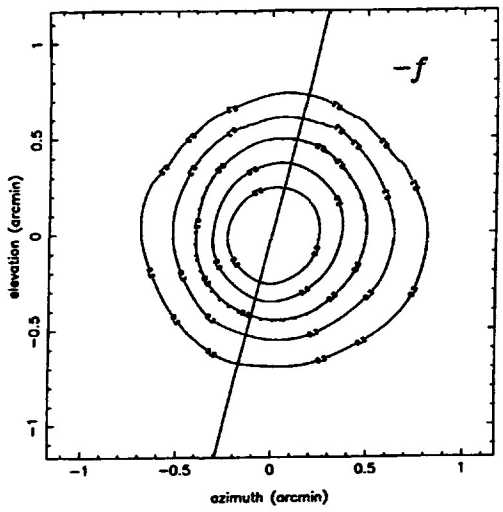

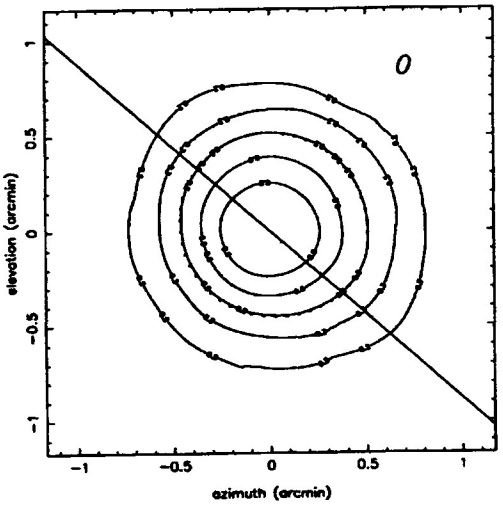

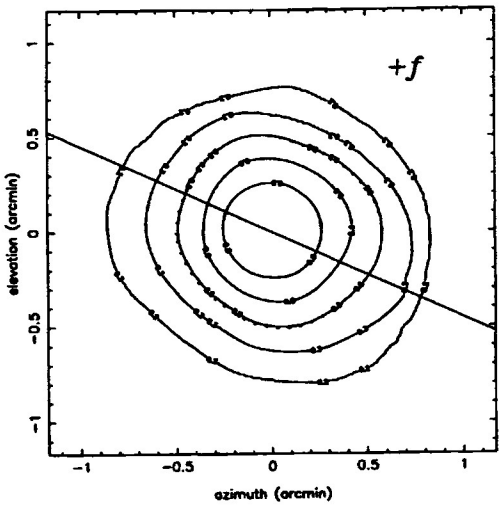

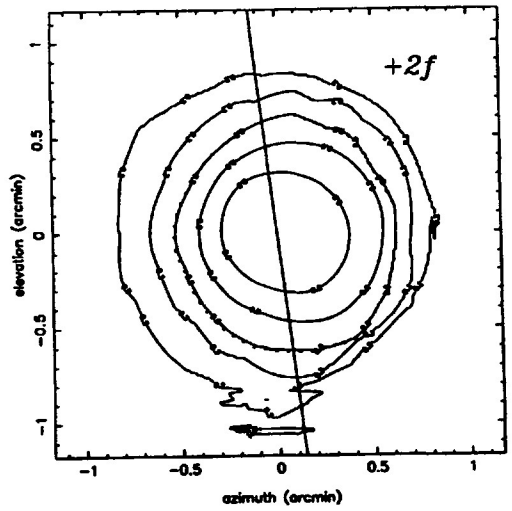

NL 7mm

x_o	y_o	a	b	ψ
+2.2	+1.9	59.5	52.8	−31.5
+2.1	+1.0	57.1	53.9	−14.1
+1.1	+1.5	59.9	57.2	+48.6
+2.1	+0.0	64.4	58.6	+65.7
+3.4	−1.6	74.1	68.0	+6.7

Figure 2q: Beam maps for NL at 7 mm.

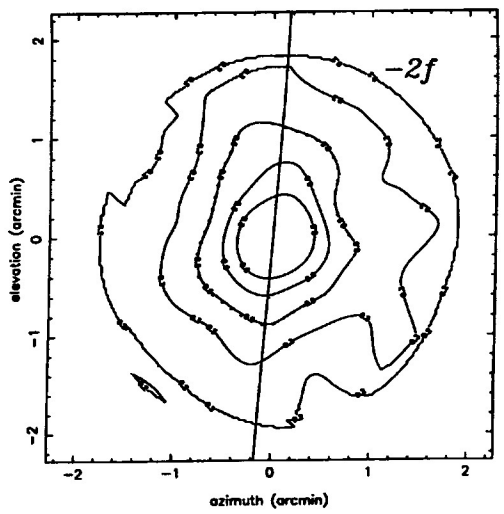

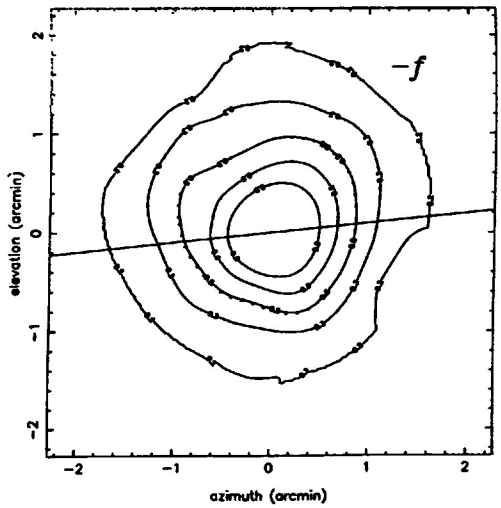

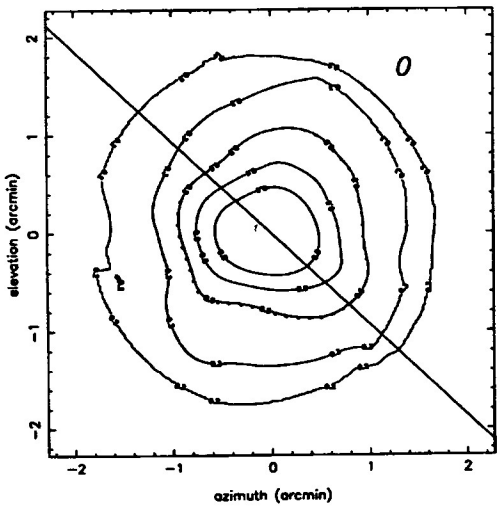

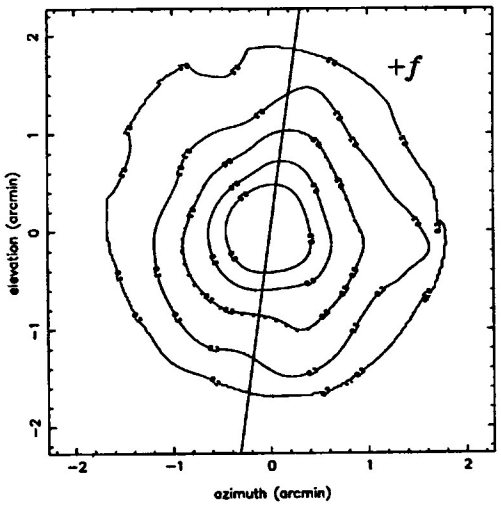

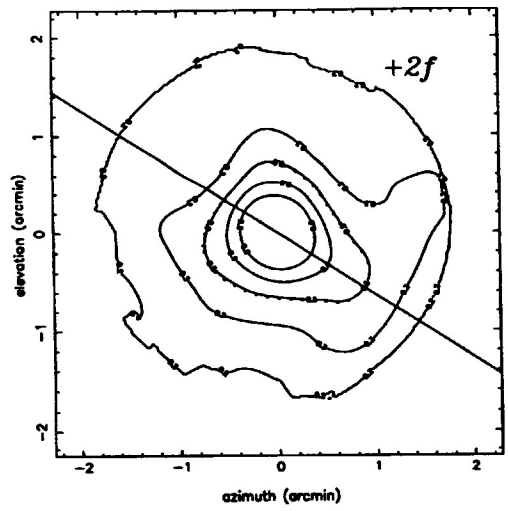

HN 1.3cm

x_o	y_o	a	b	ψ
+0.3	+6.2	120.9	89.1	−4.3
−0.1	+5.0	110.4	104.3	−84.3
+3.7	+2.4	118.4	114.2	+47.0
+1.9	−2.0	117.5	106.2	−7.9
+3.1	−4.7	102.7	76.2	+57.6

Figure 2r: Beam maps for HN at 1.3 cm.

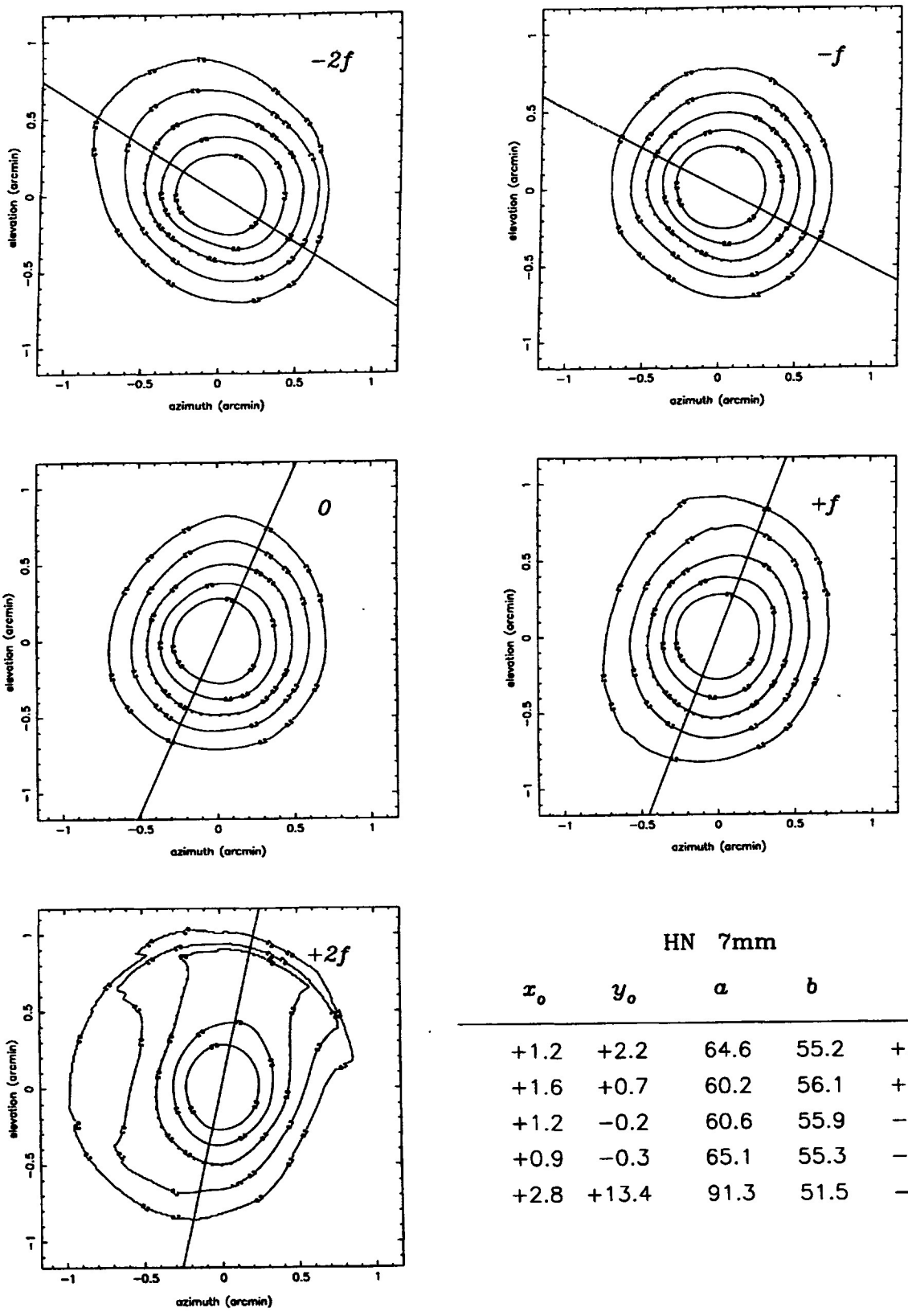

HN 7mm

x_o	y_o	a	b	ψ
+1.2	+2.2	64.6	55.2	+57.6
+1.6	+0.7	60.2	56.1	+62.6
+1.2	−0.2	60.6	55.9	−23.8
+0.9	−0.3	65.1	55.3	−21.2
+2.8	+13.4	91.3	51.5	−12.4

Figure 2s: Beam maps for HN at 7 mm.

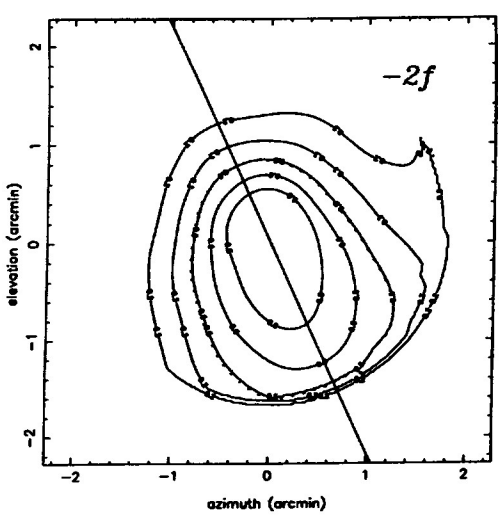

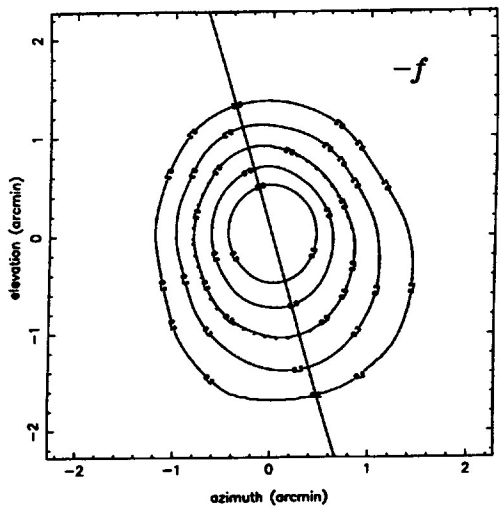

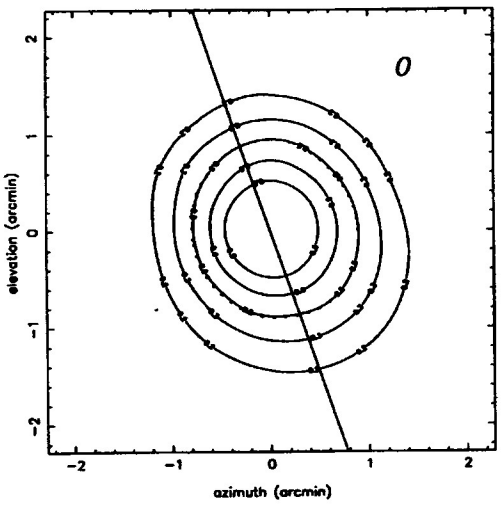

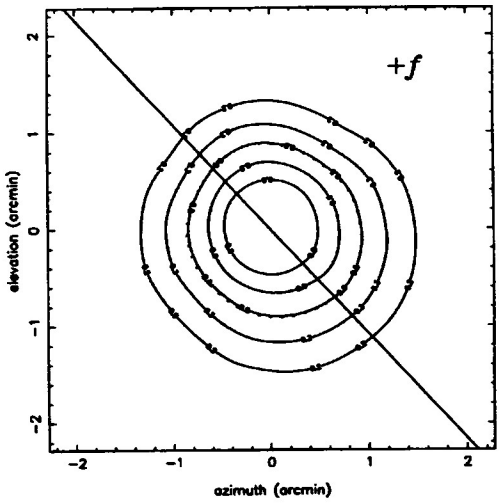

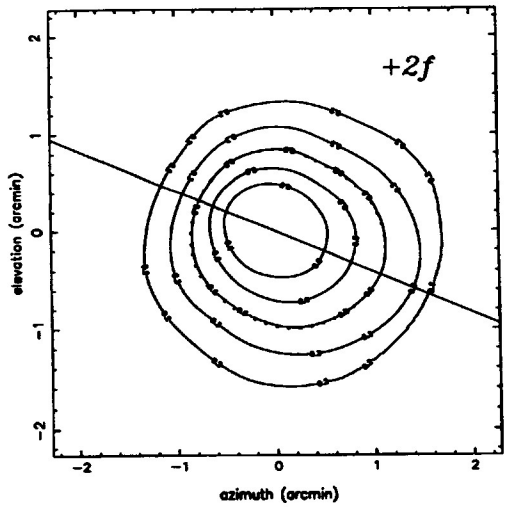

SC 1.3cm

x_o	y_o	a	b	ψ
+9.1	−25.0	150.7	112.4	+24.6
+0.0	−5.0	118.9	96.8	+16.3
+2.8	+0.4	111.9	100.2	+18.9
+2.4	−1.6	110.4	103.6	+42.8
+7.0	−5.5	120.4	106.5	+67.4

Figure 2t: Beam maps for SC at 1.3 cm.

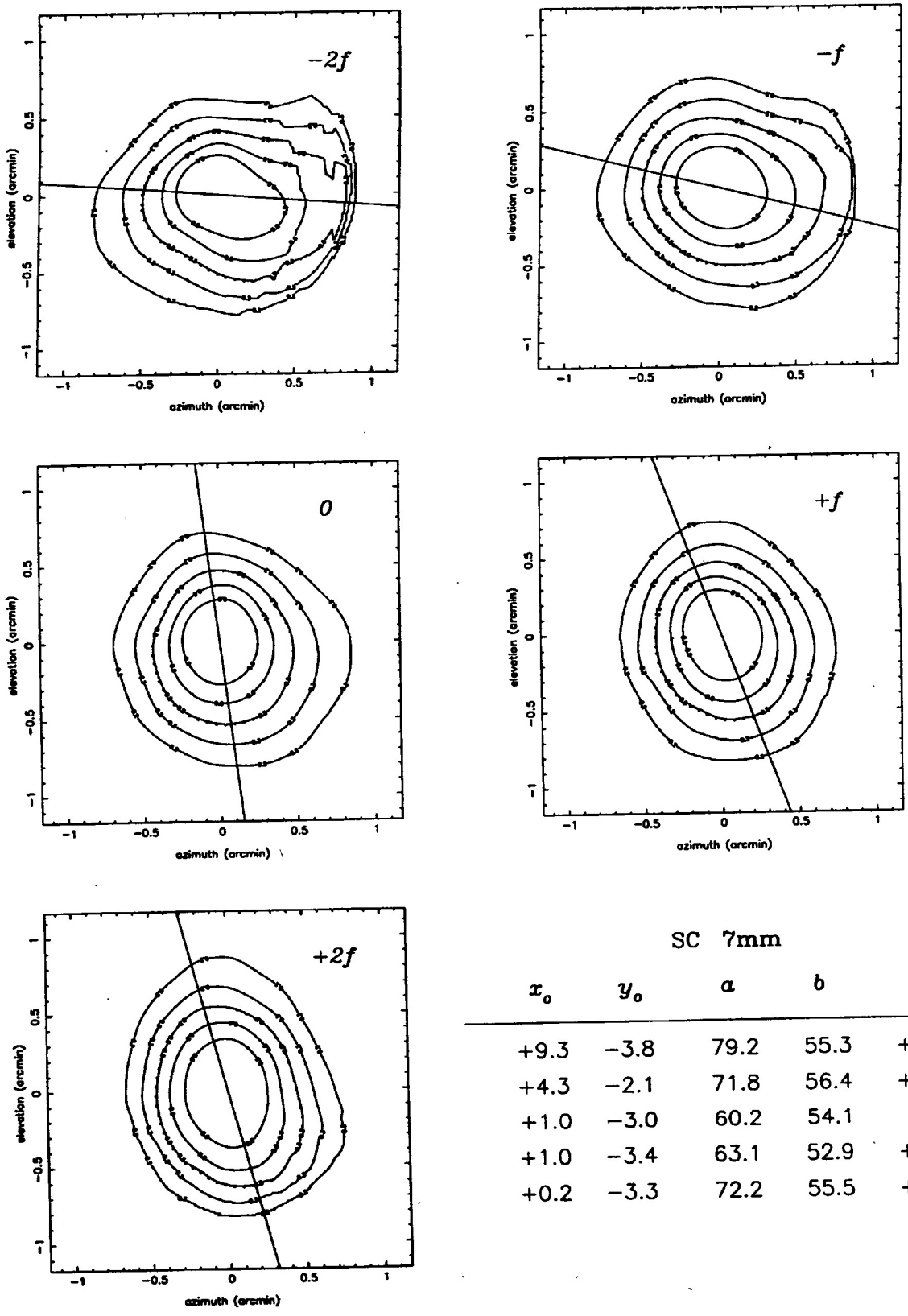

SC 7mm

x_o	y_o	a	b	ψ
+9.3	−3.8	79.2	55.3	+85.7
+4.3	−2.1	71.8	56.4	+76.1
+1.0	−3.0	60.2	54.1	+7.2
+1.0	−3.4	63.1	52.9	+20.5
+0.2	−3.3	72.2	55.5	+15.0

Figure 2u: Beam maps for SC at 7 mm.